JOURNAL OF GEOPHYSICAL RESEARCH, VOL. 106, NO. A12, PAGES 29,797–29,806, DECEMBER 1, 2001

Correlation studies of compressional Pc5 pulsations in space and Ps6 pulsations on the ground

A. Vaivads,[1,2] W. Baumjohann,[1] E. Georgescu,[1] G. Haerendel,[1]
R. Nakamura,[1] M. R. Lessard,[3] P. Eglitis,[4] L. M. Kistler,[5] and R. E. Ergun[6]

Abstract. Compressional Pc5 pulsations in space and Ps6 pulsations on the ground are common features observed in the morning sector. Here we use a conjunction study of Equator-S, Geotail, and ground stations in Canada to show that Ps6 pulsations can be the ground counterpart of compressional Pc5 pulsations observed by satellites. Because strong Ps6 pulsations are associated with optical omega-band signatures, we also suggest that the omega-band counterparts in space might be compressional pulsations on the Pc5 scale. We also discuss the magnetic field configuration that makes all these observations consistent.

1. Introduction

Strong compressional Pc5 pulsations, variations in the magnetic field amplitude with periods of typically ~10 min, are commonly observed in the outer magnetosphere at low geomagnetic latitudes. Statistical studies of spacecraft data [*Hedgecock*, 1976; *Anderson et al.*, 1990; *Takahashi et al.*, 1990; *Zhu and Kivelson*, 1991; *Haerendel et al.*, 1999; *Lessard et al.*, 1999] show that compressional Pc5 pulsations are common at large distances, $L \geq 8$, have the highest occurrence rates in the morning and afternoon sectors, and are polarized close to the meridian plane with comparable compressional and transverse components. The frequency of these pulsations is usually in the Pc5 range but can extend also to lower frequencies. The typical azimuthal size is 0.5-5 R_E ($m \approx$15–70). The radial scale size usually is larger than the azimuthal. The magnetic equator is a node for the compressional component and an antinode for the transverse component; that is, the pulsations are antisymmetric with respect to the equator (even mode) [*Takahashi et al.*, 1987; *Zhu and Kivelson*, 1994]. The pulsations are usually moving in the direction of the plasma flow (sunward convection) and are often related to substorm activity.

Besides the above mentioned, there are other types of compressional pulsations in the Pc5 frequency range that we will not discuss here: for example, compressional pulsations with phase velocities of the order of magnetosheath velocity observed close to the magnetopause, compressional pulsations associated with field line resonances that usually also have antisunward phase velocities [*Ziesolleck et al.*, 1996], or compressional pulsations associated with the global magnetosphere response to the variations in the solar wind pressure [e.g., *Sibeck et al.*, 1989]. There are also suggestions about an existence of compressional pulsations as cavity or waveguide modes; however, there is still no strong observational support for this. Thus with a term "compressional Pc5 pulsations" we mean only one part (though a large one) of all the different types of compressional Pc5 pulsations observed by satellites.

High-m pulsations moving sunward have been observed by ground magnetometers and radars in both the afternoon sector [*Allan et al.*, 1983; *Walker et al.*, 1983] and the morning sector [*Gustafsson et al.*, 1981; *Andre and Baumjohann*, 1982; *Opgenoorth et al.*, 1983; *Walker and Nielsen*, 1984]. They are denoted Ps6 pulsations (or at times Pi3), and a review of their properties has been given by *Saito* [1978]. Omega bands are the optical counterpart of strong Ps6 pulsations in the morning sector. Usually, Ps6 pulsations are associated with substorm activity or the periods of steady magnetospheric convection. They have periods 5–40 min and the amplitude of magnetic field variation is some 10 to several hundred nT [e.g., *Saito,* 1978; *Solovyev et al.,* 1999]. Ps6 pulsations tend to be observed in the east-west component of the magnetic field in the narrow, ~ 4°, latitude interval in the vicinity of the auroral electrojet current. When data are available, the pulsa-

[1]Max-Planck-Institut für extraterrestrische Physik, Garching, Germany.
[2]Now at Swedish Institute of Space Physics, Uppsala Division, Uppsala, Sweden.
[3]Thayer School of Engineering, Dartmouth College, Hanover, New Hampshire.
[4]Swedish Institute of Space Physics, Uppsala Division, Uppsala, Sweden.
[5]Space Science Center, University of New Hampshire, Durham, New Hampshire.
[6]Laboratory for Atmospheric and Space Physics, University of Colorado, Boulder, Colorado.

Paper number 2001JA900042.
0148-0227/01/2001JA900042$09.00

tions are observed concurrently at a pair of conjugate stations. Polarization of Ps6 tends to be right-handed in the premidnight (postmidnight) hours on the poleward (equatorward) side of the auroral electrojet, while left-handed in the premidnight (postmidnight) hours on the equatorward (poleward) side of the auroral electrojet. Case studies show that Ps6 pulsations move in the azimuthal direction with the background convection velocity [*Gustafsson et al.*, 1981; *Andre and Baumjohann*, 1982]. The combination of radar and magnetometer data have made it possible to develop detailed ionospheric models of Ps6 pulsations [*Buchert et al.*, 1990; *Wild et al.*, 2000, and references therein].

The similarity between the properties of the compressional pulsations seen in space and Ps6 pulsations seen on the ground has been noted already by *Saito* [1978]. There are a few case studies that explore the correlation of compressional pulsations in space and ground observations [e.g., *Lanzerotti and Tartaglia*, 1972; *Allan et al.*, 1983; *Ziesolleck et al.*, 1996]. One of the reasons for so few case studies is that compressional Pc5 waves at synchronous orbit, where many studies have been carried out, often do not have a ground signature [*Barfield et al.*, 1972]. However, this can be the result of the ionospheric shielding. The case studies indicate that compressional pulsations at synchronous orbit tend to have smaller wavelengths than at larger distances, where m numbers can be of the order 30 and less [*Takahashi et al.*, 1985; *Haerendel et al.*, 1999]. For m values of ~30 (ionospheric wavelength of ~500 km) the ionospheric shielding is not so important, and we can look for ground signatures.

The event that we use in this article to study ground-space correlation has been previously described and analyzed by *Haerendel et al.* [1999] and *Vaivads et al.* [2000]. However, ground-space correlation has not been investigated. Here we confirm that compressional Pc5 pulsations observed by Equator-S and Geotail do have corresponding Ps6 type waves on the ground. We show that the location of the pulsations is at the inner half of the plasma sheet. Finally, we give a physical model which is consistent with both space and ground observations.

2. Instrumentation

For our studies we use data from the satellites Equator-S, Geotail, and Fast Auroral Snapshot Explorer (FAST), from ground magnetometers, and the Super Dual Auroral Radar Network (SuperDARN).

From Equator-S we use data from the magnetic field instrument [*Fornacon et al.*, 1999] and the Ion Composition Instrument (ICI) [*Kistler et al.*, 1999]. From the magnetic field instrument we use 1.5-s-averaged data. While ICI, in general, measures three-dimensional (3-D) distribution functions of the major ion species in the energy range 20–40,000 eV/e, for our study we use only proton moment data. These moments are calculated from full velocity distributions obtained each 12 s. From Geotail we use 12-s-averaged data from the Geotail magnetic field [*Kokubun et al.*, 1994].

FAST has the capability to measure 3-D ion and electron distributions and electric and magnetic fields [*Carlson et al.*, 1998]. From FAST we use 2-s averages of data from the electron electrostatic analyzer (EESA) and ion electrostatic analyzer (IESA), which measure full pitch angle distributions in the sweep time of the detector (78 ms). We also use DC data from the magnetic and electric field instruments.

The Iceland West radar, located in Stokkseyri (63.86° N, 22.02° W geographic), is one of the SuperDARN HF radars [*Greenwald et al.*, 1995; *Villain et al.*, 1987]. The radars form 16 beams of separation 3.24°. In standard operation each beam is gated into 70 range cells of 45-km length, beginning at a start range of 180 km. A dwell time of 7 s is employed for each beam direction, implying that all beam directions are sampled in just under 2 min. A full scan encompasses 52° in azimuth and 3000 km in range. The Stokkseyri radar field of view extends over Greenland and the eastern edge of Canada (see Figure 2). Beam 4 is located over the magnetometer station of Iqaluit. The SuperDARN radars are sensitive to scatter from field-aligned plasma irregularities in both the F region and the E region. The measured backscatter power and irregularity phase velocities can both be employed as sensitive indicators of magnetospheric pulsations such as those related to omega bands [*Wild et al.*, 2000].

3. General Event Description

The March 9, 1998, event of compressional Pc5 pulsations occurred in the dawn sector. To characterize the location of the relevant ground stations and satellites during our event, we plot their mapping along the model magnetic field (Tsyganenko 89) into the equatorial plane of the SM coordinates (Figure 1) and onto the ground (Figure 2). During this period Equator-S and Geotail are close to but on opposite sides of the equatorial plane (the maximum distance from the equator is 1.5 R_E for Geotail and 2.5 R_E for Equator-S). The conjunction of Equator-S and Geotail is at ~1215 UT (the satellites are at the same longitude in SM coordinates). In Figure 1 we also plot the mapping of the FAST orbit 6115 during which FAST is in conjunction with Equator-S satellite at ~1615 UT. The comparison of FAST and Equator-S data will allow us to show some possible errors of the field mapping. In Figure 2, in addition, we show the field of view of the Stokkseyri radar.

March 9, 1998, was a geomagnetically quiet day with AE index values below 200 nT and Kp index between 0+ and 1+. The interplanetary magnetic field (IMF) turned southward ($Bz \approx -3$ nT, $By \approx 5$ nT) at ~0700 UT. As a result, magnetospheric convection continuously increased. At ~0820 UT substorm onset oc-

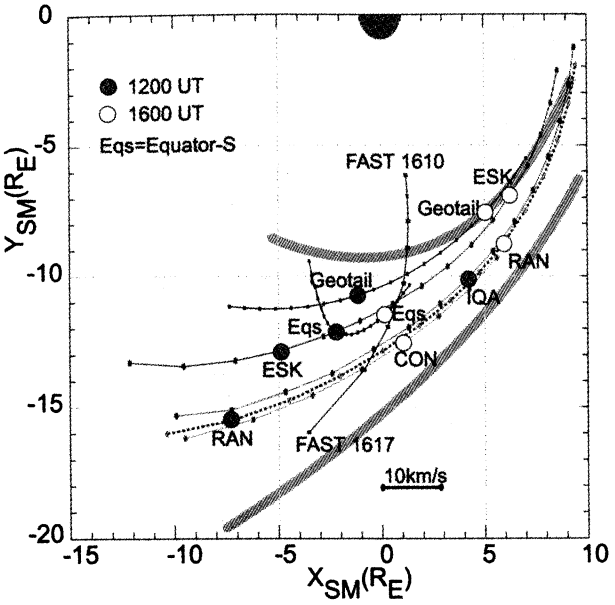

Figure 1. The mapping of ground stations Eskimo Point (ESK), Rankin Inlet (RAN), Contwoyto Lake (CON) and Iqaluit (IQA), as well as satellites Equator-S, Geotail, and Fast Auroral Snapshot Explorer (FAST) into the equatorial plane of SM coordinates. The mapping is along the Tsyganenko 89 model magnetic field. The time step for the FAST satellite is 1 min, and for the rest it is 30 min (the distance that a point with velocity 10 km/s makes in 30 min is marked "10 km/s"). The points of mapping of the ground stations, Equator-S, and Geotail move eastward (from the left to the right). The locations of satellites and ground stations at 1200 UT are marked with shaded circles, and those at 1600 UT are marked with open circles. Approximate locations of the inner boundary of the plasma sheet (from the satellite data) and the magnetopause are marked by shaded thick lines.

curred followed by later onsets (or intensifications) at 0925, 1010, and 1100 UT. After the onset of the first substorm, Equator-S and Geotail start to observe variations in magnetic field amplitude with period 5–10 min.

Figure 3 shows magnetic field observations of Equator-S and Geotail. Both satellites observe compressional pulsations for many hours. Geotail ceases to see pulsations after 1500 UT as it enters deeper into the magnetosphere. From Figure 1 it is seen that in comparison to Geotail, Equator-S moves more slowly and stays longer in the dawn sector. Equator-S observes pulsations until 1735 UT when there is an end of the data transmission.

Figure 3 shows that during the conjunction of Equator-S and Geotail the magnetic field amplitudes are in antiphase while the radial components are in phase. During the event, Equator-S is located above the equatorial plane, and Geotail is below the equatorial plane. This confirms that compressional pulsations in this data set are antisymmetric with respect to the equator [*Haerendel et al.*, 1999]. In the string picture it would correspond to an even-mode wave (second harmonic). The azimuthal wavelength of pulsations is

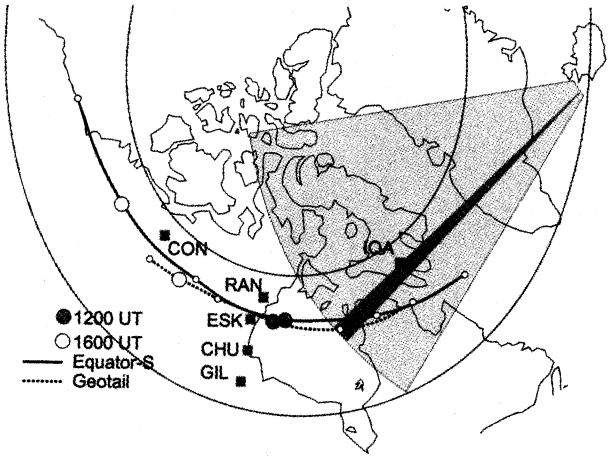

Figure 2. The orbits of Equator-S (thick solid line) and Geotail (dotted line) mapped along the model magnetic field to the ground. As in Figure 1, location of satellites at 1200 UT is marked with shaded circles and those at 1600 UT are marked with open circles. In addition, the field of view of the Stokkseyri radar and the beam 4 is shown. The lines of constant geomagnetic latitude of 65° and 75° are shown by thin lines. For the magnetic field model and ground station abbreviations, see caption of Figure 1.

$\sim 10°$ or $m \approx 30$ [*Haerendel et al.*, 1999]. For a two-dimensional (2-D) sketch of the structure of compressional pulsations, see, for example, Figure 8 of *Takahashi et al.* [1987].

During the satellite conjunction the azimuthal phase velocity of the pulsations is ~20 km/s eastward (sunward) as obtained both from the conjunction of Equator-S and Geotail [*Haerendel et al.*, 1999] and the finite gyroradius method [*Vaivads et al.*, 2000]. This is approximately the same as the mean value of the total plasma velocity (18 km/s) during this period. It was noted by *Vaivads et al.* [2000] that during this period

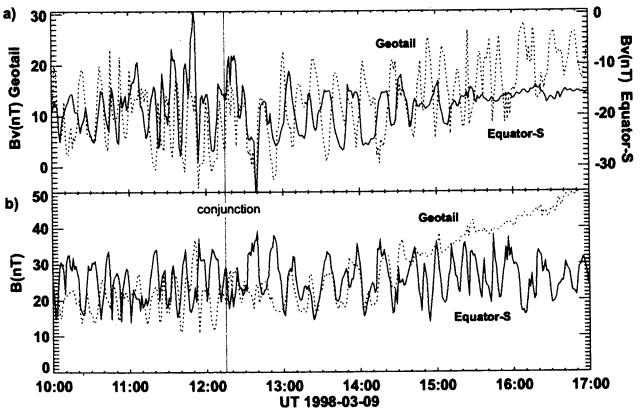

Figure 3. The magnetic field observations by Equator-S (solid line) and Geotail (dotted line): (a) B_V, the radial component of the magnetic field in SM coordinates, and (b) B, the magnetic field amplitude. During this period, Equator-S is above and Geotail is below the equatorial plane (the maximum distance from the equator is 1.5 R_E for Geotail and 2.5 R_E for Equator-S).

the contribution from large-scale magnetization current is smaller than 5 km/s, and thus the $\mathbf{E}\times\mathbf{B}$ velocity dominates the total plasma velocity. It was also shown that the phase velocity of the compressional pulsations is dominated by the azimuthal component. Summarizing, the compressional pulsations are antisymmetric structures that move approximately with the $\mathbf{E}\times\mathbf{B}$ velocity in an azimuthal direction eastward.

4. Ground Observations

In this section, using FAST and Equator-S conjunction, we first discuss the mapping using the Tsyganenko magnetic field model for our event. Then we show that Ps6 pulsations are the ground counterpart of the compressional Pc5 pulsations in space. We compare in detail the ground signatures from the magnetic stations Iqaluit and Contwoyoto Lake, the Stokkseyri radar, and the Equator-S and Geotail satellites.

4.1. Mapping Along Magnetic Field Lines

We can use data from the FAST satellite during our event to study how good the magnetic field model is for the mapping between the magnetosphere and the ionosphere. By estimating errors of the mapping from the outer magnetosphere down to FAST altitudes (4000 km), we assess fairly well the errors of the mapping from the magnetosphere down to 100-km altitude.

FAST crosses the sunward convection region (plasma sheet) almost perpendicularly. Plate 1 shows one such crossing during our event when there is a conjunction between FAST and Equator-S. The FAST data allow us to identify Region 1 and Region 2 Birkeland currents (from the eastward component of the magnetic field), the plasma sheet (from energy spectra of precipitating ions), and the boundary of trapped energetic electrons at ~1614:30 UT. Plate 1 also shows where Equator-S maps onto the FAST orbit if we use the magnetic field model. It can be seen that Equator-S maps to the inner boundary of the plasma sheet approximately at the border of the trapped energetic electron population (electrons with energies of a few keV and up).

First we check whether the mapping is consistent when we compare the ion spectra at FAST and Equator-S (~1614:40 UT is a predicted time of conjunction of both satellites). The comparison is done in Plate 2, where we plot differential energy flux of ions from both satellites. We want to find the time period along the FAST orbit when its ion spectra best fit the ion spectra seen by Equator-S. Note that FAST crosses different plasma regions within a few minutes while Equator-S stays in the same region for hours, see Figure 1. We compare the field-aligned flux intensities at Equator-S with the intensity of flux perpendicular to the ambient magnetic field at FAST (ions that move perpendicular to the ambient magnetic field at FAST altitude are almost field aligned at Equator-S). The comparison of intensities cannot be applied for ions that are heated at altitudes below FAST. Their flux intensity at Equator-S distances will be smaller by a factor of the ratio between magnetic field magnitudes at FAST and Equator-S (if there is no additional heating between FAST and Equator-S). Such heated ions with energies around 10 eV are observed by FAST around 1615 UT and at ~1615:25 UT (the pitch angle distribution to confirm this is not shown).

First thing we can note is that the ion spectrum at Equator-S for ions with energies above 1 keV corresponds well to the FAST data between ~1614:40 and ~1616:00 UT. On the other hand, the Equator-S sees a distinct ion component with energies around 100 eV. Such ions with similar intensities are seen by FAST before ~1615:30 UT but not afterward (these low-energy ions are seen also on the next orbit 2 hours later). The small difference in peak energies can be attributed to the small potential difference between magnetosphere and ionosphere. Thus, in a time interval ~1614:40–1615:30 UT the ion spectra seen by FAST fit best the ion spectra observed by Equator-S. Within this interval, FAST moves from lower to higher geomagnetic latitudes, and therefore the predicted time of conjunction ~1614:40 UT corresponds to the side of lower geomagnetic latitudes. However, Equator-S continues to see similar ion spectra for more than an hour as it moves to lower geomagnetic latitudes. Figure 1 shows that the distance covered by Equator-S within such a period corresponds to ~30 s along FAST orbit. Thus data suggest that the conjunction between FAST and Equator-S is at ~1615:10 UT or later. In other words, the data suggest that FAST maps to closer distances in the equatorial plane than is predicted by the model. It suggests that during our event also the ground stations should map in the equatorial plane slightly closer to the Earth than is predicted by the model.

4.2. Ground and Space Data Comparison

When comparing space and ground data, we cannot directly compare their frequency spectrum, because of the Doppler shifts. The point that represents the mapping of the ground stations into the equatorial plane moves with an azimuthal velocity (~5 km/s) that is larger than the azimuthal velocity of Geotail (~2.8 km/s) and Equator-S (~1 km/s). Therefore ground stations will see eastward moving pulsations at lower frequency than Geotail (which in its turn observes pulsations at lower frequency than Equator-S). Because the phase velocity of the compressional Pc5 pulsations is approximately the same as the convection velocity, the relative Doppler shifts will be larger for smaller convection velocities. For example, if the convection velocity is 20 km/s (as it is during the conjunction of Equator-S and Geotail), the frequency seen on the ground will be lower than the frequency seen by Geotail by ~10 % and it will be lower than the frequency seen by Equator-S by ~20 %. However, if the convection velocity is ~10 km/s (as it is seen after ~1630 UT by Equator-S), the ground

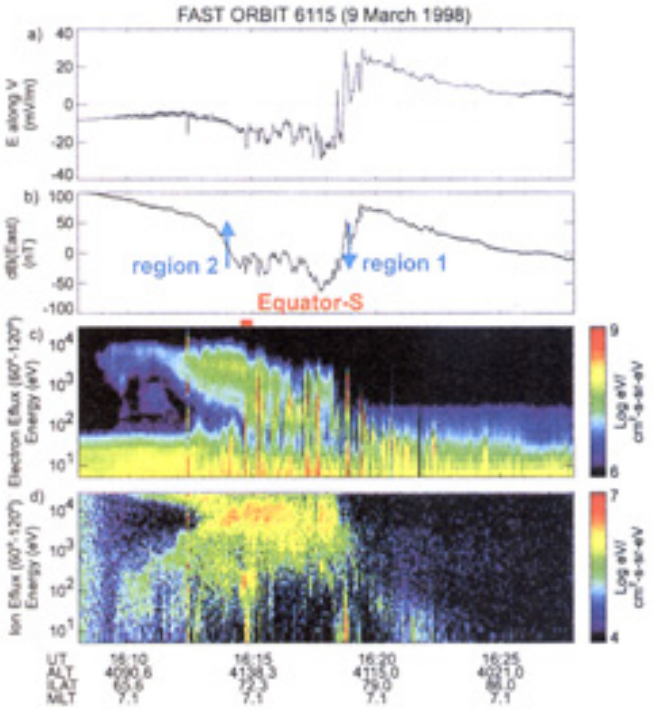

Plate 1. Data from FAST orbit 6115 crossing of the morning sector. (a) Electric field along the velocity vector (approximately north-south), (b) difference between magnetic field and model, (c) electron energy spectrogram, and (d) ion energy spectrogram. Marked are regions of Birkeland Region 1 and Region 2 currents and also the location of mapping Equator-S.

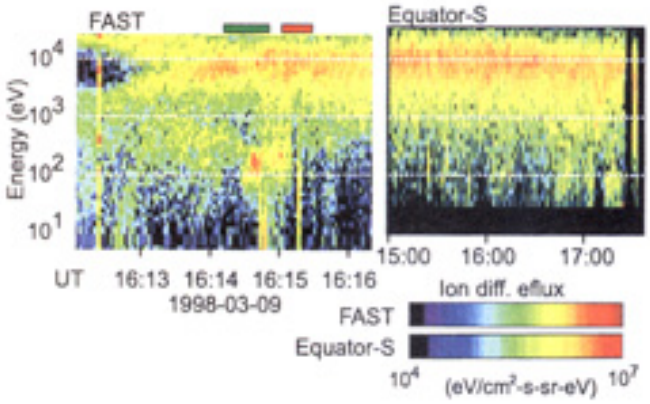

Plate 2. Comparison of the FAST ion spectrogram with the Equator-S ion spectrogram. The Equator-S ion spectrogram is obtained integrating ions from the most field aligned sectors. The region where Equator-S maps in the FAST spectrogram is marked green when derived from the magnetic field model and is marked red when derived from the comparison of ion data.

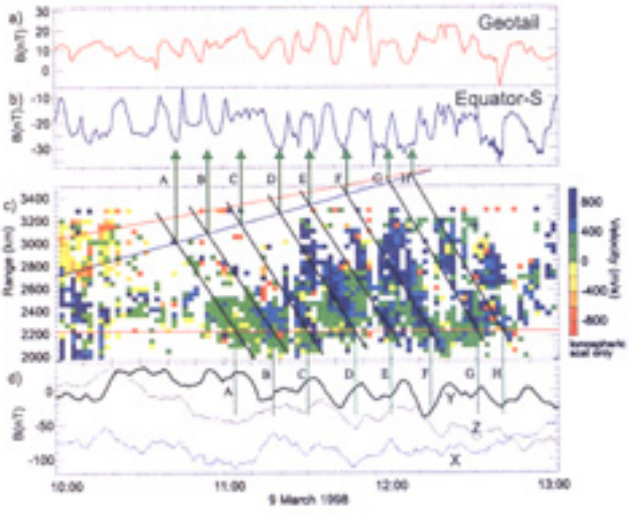

Plate 3. (a) The radial outward component in SM coordinates of the magnetic field as measured by Geotail. (b) The same for Equator-S. (c) The velocity measurements of beam 4 of the Super Dual Auroral Radar Network (SuperDARN) radar Stokkseyri. (d) The Iqaluit ground magnetometer data, where we have subtracted 6950 nT from X-, -4900 nT from Y-, and 57,050 nT from the Z component. In addition, Plate 3c has a red guideline that indicates the position of the Iqaluit station, blue and red guidelines that indicate the distance of Equator-S and Geotail from the radar, black guidelines that are fits to the eastward drift seen in the radar data above the Iqaluit station, green guidelines that show the radar signal signatures in the Iqaluit data, and green arrows that show the predicted time for Iqaluit measurements to be observed by Equator-S.

frequency will differ from Geotail by ~30 %, and it will differ from Equator-S by ~50 %.

In our case we use radar data to account for the Doppler shifts. We look at the time interval 1000-1300 UT on March 9, 1998, when Stokkseyri radar (Iceland West) obtains clear signal. Figure 2 shows that in the field of view of the radar, below beam 4, is Iqaluit station. The radar beam is almost parallel to the convection direction. During this period the footpoint of the satellites is between 500 and 1500 km westward from Iqaluit. Several observations support that the Iqaluit station is located within the inner half of the sunward convection region between ~1100 and 1300 UT: the westward electrojet location, radar data, and data from FAST (FAST crosses the auroral oval close to Iqaluit at ~1150 UT). On the other hand, Figure 1 suggests that Iqaluit is in the middle or outer half of the convection region. This discrepancy can be resolved if one takes into account our previous conclusion that ground stations most probably are mapping to closer distances than those predicted by the model. Because Equator-S during this period is also within the inner half of the convection region, we can look for a correlation between magnetometer data from Iqaluit and the Equator-S and Geotail satellites.

All the relevant data are summarized in Plate 3. Velocity data from beam 4 indicate eastward moving structures with a phase velocity of ~0.6 km/s above the ground station Iqaluit. When mapped along the magnetic field lines, this corresponds to a velocity of ~1.2 km/s at FAST altitude and ~18 km/s in the equatorial plane. These values are consistent with the plasma velocity measured at Equator-S and the $\mathbf{E}\times\mathbf{B}$ velocity at FAST. Iqaluit shows Ps6 type pulsations (best seen in the Y component), which correlate with signatures in the radar data. The green guidelines coincide with periods of increased eastward velocities in the radar data above Iqaluit, and they correlate with periods of increase in the Y-component of the ground magnetometer data (this is a characteristic of Ps6 pulsations). We use the fitting to eastward drift in the radar data (black guidelines) and estimates of the Equator-S and Geotail distance along the auroral oval from the radar (blue and red guidelines at the top of Plate 3c) to estimate the predicted times when the signatures at Iqaluit (green guidelines) are expected to be seen in the Equator-S data (green arrows). For easier discussion we have marked the green guidelines from A to H. The eastward drift in the radar data can be best seen for the black guidelines C-F. The black guidelines A, B, G, and H are not from direct fitting but just parallel to the guidelines of C–F.

Even though Plate 3 suggests a close correlation between compressional pulsations on the satellites and Ps6 pulsations on the ground, it also shows difficulties of one-to-one identification of pulsations. Thus the guideline E corresponds to two wavelengths in the Equator-S data. We can speculate that in this case we do not resolve the presence of a second pulsation event in the ground data (for this guideline there is a double peak in the Z component of the magnetic field). Guidelines A–C predict pulsations in space with a larger period than that observed by Equator-S. This also can be a result of the development of pulsations in time or the magnetometer and the radar missing or unresolving some pulsation. From Plate 3 we also cannot distinguish the phase relationship between the pulsations on the ground and the pulsations in space.

From Figure 2 we see that after 1200 UT we expect conjunctions between Equator-S and other ground stations. At ~1230 UT there is a conjunction between Equator-S and Rankin (RAN) and Eskimo (ESK) stations and at ~1500 UT there is a conjunction between Equator-S and Contwoyto Lake (CON) station. It is important to note that the time of conjunction is dependent on the magnetic field models. Thus the comparison shows that the magnetic field as observed by Equator-S is more tailward stretched than is predicted by the model (not shown). Choosing model parameters so that they better fit the magnetic field at Equator-S can shift the conjunction between CON station and Equator-S by more than a half hour (to ~1530 UT and later). Around the conjunction at 1230 UT there are no clear Ps6 type pulsations in ground magnetometer data, therefore we do not show this conjunction. We shortly comment on the ~ 1500 UT conjunction but do not go into deeper studies, because of the lack of an independent check (either by radar data or by longitudinally closely spaced stations) of the eastward motion of the observed Ps6 pulsations.

For the conjunction around ~1500 UT, in Figure 4 we plot band-pass-filtered data, 7 min $< T <$ 30 min, of B_V, the radial outward component of the magnetic

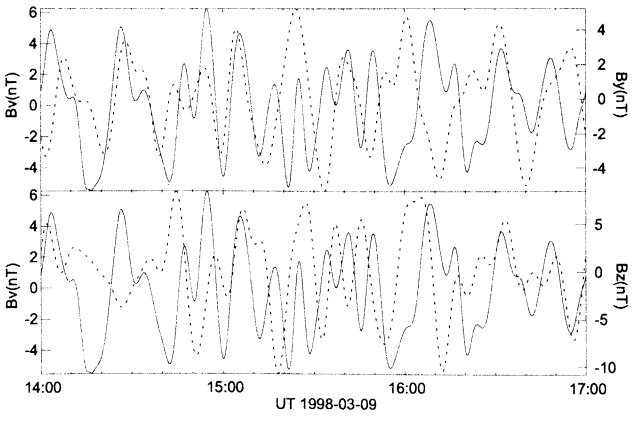

Figure 4. Band-pass-filtered data, 7 min $< T <$ 30 min, of B_V, the radial outward component of the magnetic field measured by Equator-S (solid line), and of B_Y and B_Z, the Y and Z components of the ground magnetic field (dotted line). The top panel shows B_Y, and the bottom panel shows B_Z.

field measured by Equator-S, and of B_Y and B_Z, the Y and Z components of the ground magnetic field. The pulsations seen on the ground are weak, and one-to-one identification with observations in space is not possible. Nevertheless, one can see a tendency that B_Y is in phase with B_V between ~1420 and ~1510 UT and in antiphase around 1600 UT; on the other hand, B_Z is in antiphase with B_V between ~1530 and ~1550 UT. The difficulty of one-to-one identification of pulsations can be related to the fact that Contwoyto Lake during the conjunction crosses the auroral electrojet and thus covers latitudinally slightly different regions of the plasma sheet. Also, the particular event is not a clear and strong Ps6 pulsation event; there can be superposed pulsations of an other character.

5. Results and Discussion

In this article we show that compressional Pc5 pulsations seen in the morning sector by Equator-S and Geotail are correlated with Ps6 type pulsations seen by ground magnetometers and the SuperDARN radar. The phase velocity of the pulsations is approximately equal to the velocity of plasma convection; thus the pulsations are waves approximately fixed in the plasma reference frame.

The structure of the compressional Pc5 pulsations in space and Ps6 pulsations on the ground are well studied, and there are good models for both of them. However, a weakness in both models continues to be the boundary conditions, that is, the magnetosphere for Ps6 pulsation models and the ionosphere for compressional Pc5 pulsations models. Some speculations on how both models fit have been done by Solovyev *et al.* [1999]. Below we want to present an alternative explanation that fits the main features of both models, Ps6 pulsations as a meandering electrojet and compressional Pc5 pulsations as antisymmetric waves (even mode) approximately fixed in the plasma reference frame.

Where Ps6 pulsations and omega bands map into the magnetosphere is still debated. In earlier studies the preferred location was the boundary between the plasma sheet and the low-latitude boundary layer. Later studies tended to the inner edge of the plasma sheet [*Pulkkinen et al.*, 1991; *Connors and Rostoker*, 1993; *Jorgensen et al.*, 1999]. There is also no consensus about the location of compressional pulsations (high m) observed in space, but recent studies indicate that the preferred location is the inner part of the plasma sheet [*Haerendel et al.*, 1999], as in our case.

As the magnetospheric source of the Ps6 pulsations (omega bands), often the Kelvin-Helmholtz instability is suggested [*Rostoker and Samson*, 1984; *Connors and Rostoker*, 1993]. This is because the shape of omega bands is similar to that of surface waves. The location of the shear in velocity has been put either at the outer or inner edge of the plasma sheet. Another source generating omega bands has been suggested by *Yamamoto et al.* [1997]: In a numerical simulation they show that omega bands form as an electrostatic interchange instability (Rayleigh-Taylor type of instability). On the other hand, if compressional Pc5 waves are the magnetospheric counterpart, then their generation usually is explained by the drift mirror instability (caused by high-β anisotropic plasma often resulting from injection of high-energy ions) [*Hasegawa*, 1969; *Baumjohann et al.*, 1987]. The model of *Yamamoto et al.* [1997] seems to be included in more advanced theories of drift mirror instability that take into account ballooning and mirroring effects and the curvature of the magnetic field [e.g., *Chen and Hasegawa,* 1994].

There are several reasons to believe that the Kelvin-Helmholtz instability alone cannot be the source of compressional pulsations (and Ps6 pulsations). Observations indicate that the compressional pulsations are seen usually inside high-β plasma when mirror conditions tend to be satisfied [*Zhu and Kivelson*, 1994]. In addition, at the inner edge of the plasma sheet there is usually no strong velocity gradient such as is required for the Kelvin-Helmholtz instability (as can be seen, for example, in the top panel of Figure 1a, where a north-south electric field corresponds to the azimuthal $\mathbf{E}\times\mathbf{B}$velocities and the inner edge of the plasma sheet coincides approximately with the Region 2 currents). What effect small-velocity shears could have on drift mirror instabilities has not been explored. Another way around the problem of small-velocity shear has been given by *Allan and Wright* [1997]. They suggest that the Kelvin-Helmholtz instability could develop in regions of field line resonance, where the velocity shear can be much larger than the velocity shear in the background plasma convection. This nonlinear Kelvin-Helmholtz instability would serve as a seed for the drift mirror instability.

Another thing to note is that the theory predicts antisymmetric structure of pulsations generated by the drift mirror instability only if kinetic effects are taken into account [*Southwood*, 1976; *Cheng and Qian*, 1994]. Such effects are usually disregarded in studies applying the Kelvin-Helmholtz instability (for example, working with 2-D models), and therefore the field-aligned structure is usually not discussed, or it is assumed to be of the fundamental mode type.

Thus, assuming that the drift mirror instability generates compressional Pc5 pulsations in space, we have to suggest a model that relates these pulsations to the ground observations of Ps6 pulsations. Here we suggest one such model; the model is sketched in Figure 5, and we explain it below.

Previous studies show that the source of Ps6 pulsations is a meandering electrojet that can be caused by field-aligned currents and/or a meandering electric field [e.g., *Buchert et al.*, 1990; *Gustafsson et al.,* 1981; *Saito and Yumoto,* 1978]. Thus we want to show how compressional Pc5 pulsations can cause electrojet meandering. That compressional pulsations in space can create

parallel currents that close into the ionosphere has been shown by *Cheng and Qian* [1994]. Figure 5a shows compressional Pc5 pulsations and the field-aligned currents associated with them. Note that the total field-aligned current into the ionosphere will be different and will depend on the Region 2 field-aligned currents and conductivity gradients in the ionosphere [e.g., *Wild et al.,* 2000]. The top of the Figure shows three magnetic flux tubes as seen on the dawnside when looking from the tail. The darkest shaded flux tube is the nearest one. Flux tubes are spaced at half the azimuthal wavelength of the pulsations. The darkest shaded and the light shaded flux tubes are shifted upward with respect to the equator, and the shaded flux tube is shifted downward. This is consistent with the magnetic field configuration of compressional Pc5 pulsations [e.g., *Haerendel et al.,* 1999]. Two bottom circles show how the flux tubes end in the ionospheres of both hemispheres. We also show the direction of parallel currents and the direction in which the ends of the flux tubes will relax (as explained later).

Now we ask how the compressional pulsations relax when their energy is dumped into the ionosphere. Because of the finite conductivity of the ionosphere, field lines will tend to move in the direction that releases the magnetic stress, so that the parallel currents into the ionosphere associated with the compressional pulsations decrease. The antisymmetric structure of the pulsations

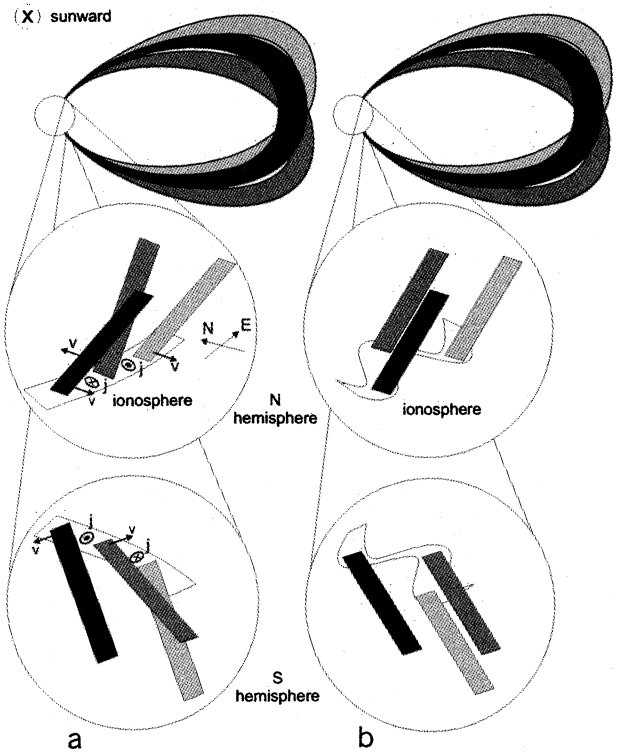

Figure 5. The magnetic field configuration of compressional pulsations and how the magnetic flux tubes map into the ionosphere: (a) case when compressional pulsations have associated with them parallel currents into the ionosphere and (b) when there are no parallel currents. The darkest shaded magnetic flux tube is the nearest.

implies that the ends of the magnetic field lines in both hemispheres will move into the same direction, north or south. Because the compressional pulsations have almost zero phase velocity with respect to the plasma, the above mentioned south or north movement of field lines will not be oscillatory (as in a poloidal Alfvén wave) but will eventually stop as the parallel currents associated with the pulsations decrease. The characteristic relaxation time for a Pedersen conductivity of 5 S would be ~10 min, which is comparable to the pulsation period. This timescale is also shorter than the life time of compressional pulsations, which has been estimated by *Haerendel et al.* [1999] to be at least 17–35 min. Note that the Region 2 Birkeland current (located at the inner edge of the plasma sheet) will still be present. Figure 5b shows the configuration of the magnetic field for a case when the parallel current associated with the pulsations has already become small because of the field line movement in the ionosphere. We can see that after relaxation the line connecting the ends of the flux tubes has become meander-like.

There are several important predictions from Figure 5b. First there are still compressional pulsations out in the magnetosphere even though there are no parallel currents into the ionosphere associated with these pulsations. That is to say, the ionospheric ends of the flux tubes have relaxed while out in the equatorial plane the flux tubes keep their initial azimuthal and antisymmetric structure. This would provide an explanation why compressional Pc5 pulsations can be observed also during geomagnetically quiet periods for a long period of time after having developed into stationary, nonpulsating structures or plasma blobs [*Haerendel et al.,* 1999]. Secondly, field lines that before mapped to the same latitude in Figure 5a, map to different latitudes in Figure 5b. Assuming that the magnetic field lines are equipotential, we see from Figure 5b that the potential in the ionosphere will form a snake-like or wave-like form similar to that of omega bands. When these "snakes" are mapped out into the magnetosphere, they will become straight lines at the equatorial plane (and they will be 180° out of phase in the ionosphere of the opposite hemisphere). The relation is such that the field line which has the radial component of the magnetic field in the equatorial plane more positive than the neighboring field line maps to higher latitudes in the Northern Hemisphere and lower latitudes in the Southern Hemisphere. Thus these field lines would map to the ground at longitudes where the omega bands have luminous tongues. Thirdly, to see the predicted correlation between the ground and space, we have to take into account the models and observations of the omega band (Ps6 pulsations). They usually show that the maximum in $D(Y)$ component of the magnetic field measured on the ground coincides with the western edge of the luminous tongue or with the luminous tongue itself [e.g., *Lühr and Schlegel,* 1994; *Solovyev et al.,* 1999]. Thus we expect that B_V, the radial component of the mag-

netic field in the equatorial plane, either will be in phase with the oscillations of the B_Y on the ground or will be phase advanced by approximately one-fourth of a wavelength. The last case predicts that B_V and B_Z will be in antiphase, because usually for Ps6 pulsations, B_Z is phase delayed with respect to B_Y by approximately one-fourth of a wavelength. Figure 4 showed that B_V and B_Y tend to be in phase shortly before 1500 UT and that B_V and B_Z are in antiphase around 1540 UT. Both these phase relationships are consistent with different omega band models, but the uncertainty of the time of conjunction (it is sensitive to the magnetic field model and can be between 1500 and 1530 UT) does not allow us to distinguish which is a case. Additional studies are required to confirm or disprove the proposed model and its predicted phase relationships between the ground and space.

From the above reasoning it also follows that the presence of compressional pulsations in the space is not a sufficient condition for the existence of the Ps6 pulsations on the ground; there also must be an increased electrojet. Thus Ps6 pulsations will be associated with substorm activity (or a period of steady magnetospheric convection) while compressional pulsations in space can be seen a long time after substorm activity has died out.

Acknowledgments. The authors thank the FAST team for supplying FAST data. The CANOPUS instrument array, constructed and operated by the Canadian Space Agency, provided some of the data used in this study. Magnetic field data from ground station Iqaluit are supplied by the Geological Survey of Canada.

Michel Blanc thanks A. David M. Walker and Mark J. Engebretson for their assistance in evaluating this paper.

References

Allan, W., and A. N. Wright, Large-m waves generated by small-m field line resonances via the nonlinear Kelvin-Helmholtz instability, *J. Geophys. Res., 102*, 19,927–19,933, 1997.

Allan, W., E. M. Poulter, K.-H. Glassmeier, and E. Nielsen, Ground magnetometer detection of a large-m Pc 5 pulsation observed with the STARE radar, *J. Geophys. Res., 88*, 183–188, 1983.

Anderson, B. J., M. J. Engebretson, S. P. Rounds, L. J. Zanetti, and T. A. Potemra, A statistical study of Pc 3-5 pulsations observed by the AMPTE/CCE magnetic fields experiment, 1, Occurrence distributions, *J. Geophys. Res., 95*, 10,495–10,523, 1990.

Andre, D., and W. Baumjohann, Joint two-dimensional observations of ground magnetic and ionospheric electric-fields associated with auroral currents, 5, Current system associated with eastward drifting omega bands, *J. Geophys., 50*, 194–201, 1982.

Barfield, J. N., R. L. McPherron, P. J. Coleman Jr., and D. J. Southwood, Storm-associated Pc 5 micropulsation events observed at the synchronous equatorial orbit, *J. Geophys. Res., 77*, 143–158, 1972.

Baumjohann, W., N. Sckopke, J. LaBelle, B. Klecker, H. Luhr, and K. H. Glassmeier, Plasma and field observations of a compressional Pc 5 wave event, *J. Geophys. Res., 92*, 12,203–12,212, 1987.

Buchert, S., G. Haerendel, and W. Baumjohann, A model for the electric fields and currents during a strong Ps 6 pulsation event, *J. Geophys. Res., 95*, 3733–3743, 1990.

Carlson, C. W., R. F. Pfaff, and J. G. Watzin, The Fast Auroral Snapshot (FAST) mission, *Geophys. Res. Lett., 25*, 2013–2016, 1998.

Chen, L., and A. Hasegawa, Kinetic-theory of geomagnetic-pulsations, 2, Ion flux modulations by transverse-waves, *J. Geophys. Res., 99*, 179–182, 1994.

Cheng, C. Z., and Q. Qian, Theory of ballooning-mirror instabilities for anisotropic pressure plasmas in the magnetosphere, *J. Geophys. Res., 99*, 11,193–11,209, 1994.

Connors, M., and G. Rostoker, Source mechanisms for morning auroral features, *Geophys. Res. Lett., 20*, 1535–1538, 1993.

Fornacon, K.-H., H. U. Auster, E. Georgescu, W. Baumjohann, K.-H. Glaßmeier, J. Rustenbach, and M. Dunlop, The magnetic field experiment onboard Equator-S and its scientific possibilities, *Ann. Geophys., 17*, 1521–1527, 1999.

Greenwald, R. A., et al., DARN/SuperDARN: A global view of the dynamics of high-latitude convection, *Space Sci. Rev., 71*, 761–796, 1995.

Gustafsson, G., W. Baumjohann, and I. Iversen, Multimethod observations and modeling of the 3-dimensional currents associated with a very strong Ps6 event, *J. Geophys., 49*, 138–145, 1981.

Haerendel, G., W. Baumjohann, E. Georgescu, R. Nakamura, L. M. Kistler, B. Klecker, H. Kucharek, A. Vaivads, T. Mukai, and S. Kokubun, High-beta plasma blobs in the morningside plasma sheet, *Ann. Geophys., 17*, 1592–1601, 1999.

Hasegawa, A., Drift mirror instability in the magnetosphere, *Phys. Fluids, 12*, 2642–2650, 1969.

Hedgecock, P. C., Giant Pc 5 pulsations in the outer magnetosphere: A survey of HEOS-1 data, *Planet. Space Sci., 24*, 921–935, 1976.

Jorgensen, A. M., H. E. Spence, T. J. Hughes, and D. McDiarmid, A study of omega bands and Ps6 pulsations on the ground, at low altitude and at geostationary orbit, *J. Geophys. Res., 104*, 14,705–14,715, 1999.

Kistler, L., et al., Testing electric field models using ion energy spectra from the Equator-S ion composition (ESIC) instrument, *Ann. Geophys., 17*, 1611–1621, 1999.

Kokubun, S., T. Yamamoto, M. H. Acuna, K. Hayashi, K. Shiokawa, and H. Kawano, The Geotail magnetic field experiment, *J. Geomagn. Geoelectr., 46*, 7–21, 1994.

Lanzerotti, L. J., and N. A. Tartaglia, Propagation of a magnetospheric compressional wave to the ground, *J. Geophys. Res., 77*, 1934–1940, 1972.

Lessard, M. R., M. K. Hudson, and H. Luhr, A statistical study of Pc 3-Pc 5 magnetic pulsations observed by the AMPTE/Ion Release Module satellite, *J. Geophys. Res., 104*, 4523-4538, 1999.

Luhr, H., and K. Schlegel, Combined measurements of EISCAT and the EISCAT magnetometer cross to study omega bands, *J. Geophys. Res., 99*, 8951–8959, 1994.

Opgenoorth, H.J., J. Oksman, K.U. Kaila, E. Nielsen, and W. Baumjohann, Characteristics of eastward drifting omega-bands in the morning sector of the auroral oval, *J. Geophys. Res., 88*, 9171–9185, 1983.

Pulkkinen, T. I., R. J. Pellinen, H. E. J. Koskinen, H. J. Opgenoorth, J. S. Murphree, V. Petrov, A. Zaitzev, and E. Friis-Christensen, Auroral signatures of substorm recovery phase: A case study, in Magnetospheric Substorms, *Geophys. Monogr. Ser.*, vol. *64*, edited by Kan et al., pp. 333–342, AGU, Washington, DC, 1991.

Rostoker, G., and J. C. Samson, Can substorm expansive phase effects and low frequency Pc magnetic pulsations be attributed to the same source mechanism?, *Geophys. Res. Lett., 11*, 271–274, 1984.

Saito, T., Long-period irregular magnetic pulsation, Pi3, *Space Sci. Rev., 21*, 427-467, 1978.

Saito, T., and K. Yumoto, Comparison of the two-snake model with the observed polarization of the substorm-associated magnetic pulsation Ps 6, *J. Geomagn. Geoelectr.*, *30*, 39–54, 1978.

Sibeck, D. G., et al., The magnetospheric response to 8-minute-period strong-amplitude upstream pressure variations, *J. Geophys. Res.*, *94*, 2505–2519, 1989.

Solovyev, S. I., D. G. Baishev, E. S. Barkova, M. J. Engebretson, J. L. Posch, W. J. Hughes, K. Yumoto, and V. A. Pilipenko, Structure of disturbances in the dayside and nightside ionosphere during periods of negative interplanetary magnetic field B_z, *J. Geophys. Res.*, *104*, 28,019–28,039, 1999.

Southwood, D. J., A general approach to low-frequency instability in the ring current plasma, *J. Geophys. Res.*, *81*, 3340–3348, 1976.

Takahashi, K., P. R. Higbie, and D. N. Baker, Azimuthal propagation and frequency characteristic of compressional Pc 5 waves observed at geostationary orbit, *J. Geophys. Res.*, *90*, 1473–1485, 1985.

Takahashi, K., J. F. Fennell, E. Amata, and P. R. Higbie, Field-aligned structure of the storm time Pc 5 wave of November 14-15, 1979, *J. Geophys. Res.*, *92*, 5857–5864, 1987.

Takahashi, K., C. Z. Cheng, R. W. McEntire, and L. M. Kistler, Observation and theory of Pc 5 waves with harmonically related transverse and compressional components, *J. Geophys. Res.*, *95*, 977–989, 1990.

Vaivads, A., W. Baumjohann, G. Haerendel, R. Nakamura, H. Kucharek, B. Klecker, M. R. Lessard, L. M. Kistler, T. Mukai, and A. Nishida, Compressional Pc5 type pulsations in the morningside plasma sheet, *Ann. Geophys.*, *19*, 311–320, 2001.

Villain, J. P., R. A. Greenwald, K. B. Baker, and J. M. Ruohonomie, HF radar observations of E-region plasma irregularities produced by oblique electron streaming, *J. Geophys. Res.*, *92*, 12,327–12,342, 1987.

Walker, A. D. M., and E. Nielsen, Stare observations of an eastward propagating Pc5 pulsation with large azimuthal wavenumber, *Geophys. Res. Lett.*, *11*, 259–262, 1984.

Walker, A. D. M., H. Junginger, and O. H. Bauer, GEOS 2 plasma drift velocity-measurements associated with a storm time Pc5 pulsation, *Geophys. Res. Lett.*, *10*, 757–760, 1983.

Wild, J. A., T. K. Yeoman, P. Eglitis, and H. J. Opgenoorth, Multi-instrument observations of the electric and magnetic field structure of omega bands, *Ann. Geophys.*, *18*, 99–110, 2000.

Yamamoto, T., S. Inoue, and C.-I. Meng, Formation of auroral omega bands in the paired region 1 and region 2 field-aligned current system, *J. Geophys. Res.*, *102*, 2531–2544, 1997.

Zhu, X., and M. G. Kivelson, Compressional ULF waves in the outer magnetosphere, 1, Statistical study, *J. Geophys. Res.*, *96*, 19,451–19,467, 1991.

Zhu, X., and M. G. Kivelson, Compressional ULF waves in the outer magnetosphere, 2, A case-study of Pc-5 type wave activity, *J. Geophys. Res.*, *99*, 241–252, 1994.

Ziesolleck, C. W. S., Q. Feng, and D. R. McDiarmid, Pc 5 ULF waves observed simultaneously by GOES 7 and the CANOPUS magnetometer array, *J. Geophys. Res.*, *101*, 5021–5033, 1996.

W. Baumjohann, E. Georgescu, G. Haerendel, R. Nakamura, Max-Planck-Institut für extraterrestrische Physik, Garching, 85741 Germany. (e-mail: wb@mpe.mpg.de; gh@mpe.mpg.de;)

P. Eglitis, A. Vaivads, Swedish Institute of Space Physics, Uppsala Division, Box 537, SE-751 21 Uppsala, Sweden. (e-mail: andris@irfu.se)

R. E. Ergun, University of Colorado, LASP, 1234 Innovation Dr Campus, Box 530, Boulder, CO 80303.

L. M. Kistler, Space Science Center, University of New Hampshire, SSC, Morse Hall, Durham, NH 03824-3525.

M. R. Lessard, Dartmouth College, Thayer School of Engineering, 8000 Cummings Hall, Hanover, NH 03755-8000.

(Received August 16, 2000; revised January 14, 2001; accepted March 16, 2001.)